Imaging of the Lungs Using 3He MRI: Preliminary Clinical Experience in 18 Patients with and without Lung Disease

Hans-Ulrich Kauczor, MD • Michael Ebert, MS • Karl-Friedrich Kreitner, MD • Helge Nilgens, PhD
Reinhard Surkau, PhD • Werner Heil, PhD • Dirk Hofmann, MS • Ernst W. Otten, PhD
Manfred Thelen, MD

The purpose of this study was to describe the 3He MRI findings of normal pulmonary ventilation in healthy volunteers and to evaluate abnormalities in patients with different lung diseases. Hyperpolarized 3He gas (300 ml, 3 × 10^5 Pa, polarized to 35–45% by optical pumping, provided in special glass cells) was inhaled by 8 healthy volunteers and 10 patients with different lung diseases. Imaging was performed with a three-dimensional fast low-angle shot (FLASH) sequence (TR = 11.8 msec; TE = 5 msec; transmitter amplitude, 5–8 V; corresponding flip angle, <5°) in a single breath-hold (22–42 seconds). Clinical and radiologic examinations were available for correlation. The studies were performed successfully in eight of eight volunteers and in 8 of 10 patients. The lung parenchyma of volunteers with normal ventilatory function exhibited rather homogeneous intermediate to high signal, whereas patients with chronic obstructive lung disease or bronchiectasis presented with severe signal inhomogeneities with patchy or wedge-shaped defects. The mass effect of bronchogenic carcinoma, chronic empyema, lymphadenopathy, or pleural effusion caused large signal defects, representing the lesion and adjacent hypoventilation, the extent of which had not been presumed from chest x-ray or CT. 3He MRI is a promising new modality for the assessment of pulmonary ventilation and its abnormalities. Additional studies are needed to determine its potential clinical role.

Index terms: Lung, MR • MR, contrast enhancement • MR, nuclei other than H • Hyperpolarized inert gases

JMRI 1997; 7:538–543

Abbreviations: COPD = chronic obstructive pulmonary disease, FLASH = fast low-angle shot, PFT = pulmonary function test.

From the Department of Radiology (H.-U.K., K.-F.K., H.N., M.T.) and the Institute of Physics (M.E., R.S., W.H., D.H., E.W.O.), Johannes Gutenberg-University Mainz, Langenbeckstr 1, 55131 Mainz, Germany. Received October 9, 1996; revision requested December 10; revision received January 14, 1997; accepted January 17. **Address correspondence to:** H.-U.K. E-mail: kauczor@radiologie.klinik.uni-mainz.de.

MRI BASED ON HYPERPOLARIZED 3He gas is emerging as a promising modality for imaging of the lungs. The large nonequilibrium polarization in the nuclei of the hyperpolarized 3He gas represents the source of the MR signal. Unfortunately, hyperpolarized 3He is available only in gaseous form and is not soluble in water or blood. However, helium can be inhaled in considerable amounts and concentrations (80% helium, 20% oxygen) without risk, as is known from deep sea diving and special lung function tests (measurement of the residual volume). After inhalation of the hyperpolarized 3He gas, airways and alveolar airspaces can be visualized with a strong signal as has been demonstrated under experimental conditions in the guinea pig lung (1,2) and in humans (3–5). Based on this knowledge, we applied 3He MRI in healthy, nonsmoking volunteers and in patients with different lung diseases as well as smokers to assess the visualization of airspaces and their abnormalities. This study describes one of the first applications in patients with abnormal lung function. Findings were compared with clinical data, pulmonary function tests (PFT), chest x-ray, CT, and ventilation scintigraphy when available.

• MATERIAL AND METHODS

The technical prerequisites and details for production and supply of hyperpolarized 3He gas already have been reported elsewhere (6,7). In summary, hyperpolarization of 3He gas is achieved by direct optical pumping (arc-lamp pumped laser composed of $La_{.85}ND_{.15}MgAl_{11}O_{13}$) inducing multiple metastability exchange collisions to the nuclei (6). A production rate of approximately 6 × 10^{18} polarized spins per second is achievable (7). The high polarized spin density obtained (35–45%) is necessary for the clinical application of 3He MRI (3). Relaxation times with a T1 of up to 100 hours have been measured (8). The compressed hyperpolarized gas (volume, 300 ml; pressure, 3 × 10^5 Pa) is filled into special internally coated, iron-free Supremax glass cells (Schott Glaswerke, Mainz, Germany) to allow easy handling and long relaxation times. After use, the glass cell can be refilled easily and reused. For 3He MRI, the hyperpolarized 3He samples are moved rapidly (5 seconds) into the center of the magnet

to minimize polarization losses induced by the field gradients in the stray field zone.

All imaging studies were performed on a 1.5-T Magnetom Vision (Siemens Medical Systems, Erlangen, Germany). For imaging, the broadband system of the regular spectroscopic accessory of the MR system is applied. The gradient strengths are adjusted for the gyromagnetic ratio of 3He. A special transmit/receive Helmholtz coil operating at 48.44 MHz with an outer diameter of 31.5 cm and manual tuning was designed for 3He imaging. This circular coil has a double-loop design; the variable distance between the two loops ranges between 20.0 and 25.5 cm. For the MRI studies, the chest of the individuals was positioned exactly within the two loops of the Helmholtz coil because scout views were not performed. In deep inspiration, the anterior loop of the coil just made contact with the anterior chest wall. The coil is tuned manually with the subject in the center of the magnet. A three-dimensional (3D) fast low-angle shot (FLASH) sequence was applied with TR = 11.8 msec, TE = 5 msec, phase encoding from top to bottom, transmitter amplitude of 5–8 V (depending on body weight and chest size), corresponding to a flip angle of well below 5°, total receiver gain of 85 dB, matrix size of 144 × 256, field of view of 350 mm, and coronal orientation. The slab thickness and number of partitions were adapted to the breath-hold capability of the individual. Before the 3D FLASH sequence was started, the individual was familiarized with the inhalation and imaging procedure. This procedure has been described previously (3,9). Breathing of ordinary, nonpolarized 4He gas before the hyperpolarized sample is important to wash out ordinary air and oxygen from the lungs. The breath-hold capability of the individual under these circumstances is tested, and the sequence is adjusted accordingly. Breath-hold periods ranged from 22 to 42 seconds, and the slab thickness of the 3D FLASH sequence varied between 14 and 17 cm with 14–24 partitions resulting in an effective slice thickness of 7–10 mm. The matrix size had to be reduced to 128 × 256 for one patient. Maximum intensity projections (MIP) were obtained from the source images in all studies using on-line image processing software.

3He MRI was performed in eight healthy, nonsmoking volunteers (seven males, one female; mean age, 30 years; age range, 27–34 years; normal pulmonary function) and in 10 patients (eight males, two females; mean age, 57.1 years; age range, 29–70 years). Six patients were suffering from chronic obstructive pulmonary disease (COPD); two presented with bronchogenic carcinoma (one also with pleural effusion) and two presented with pneumonia. All six patients were smokers (>10 pack years). Other underlying diseases were: chronic empyema with an air-fluid level and a destroyed right lower lobe due to atypical tuberculosis (n = 1, nonsmoker), fibrosis (n = 1, nonsmoker), bihilar and mediastinal lymphadenopathy in Hodgkin's disease (n = 1, nonsmoker), and bronchiectasis (n = 1, nonsmoker). Informed consent was obtained from all patients after the procedure had been fully explained. Patients with known contraindications for MRI were not examined. The study has been approved by our regional ethics committee.

The overall success rate of 3He MRI was judged on the basis of completion of the whole inhalation and imaging procedure; the detection of the hyperintense hyperpolarized 3He gas within the lungs allowed for visual assessment of pulmonary ventilation. Source images and MIPs were visually assessed by two radiologists, and final consensus was required. The signal intensities within the upper, lower, anterior, and posterior lung fields were rated on a four-point scale as none, low, intermediate, or high. Special attention was paid to the possible influence and limitations of the Helmholtz coil (signal intensities adjacent to the coil, dependence on chest size: anterioposterior and craniocaudal distance). The severity (mild, moderate, or severe) and localization of signal inhomogeneities, as well as the presence of respiratory or cardiac motion artifacts, were noted. 3He MRI findings in patients were correlated with the underlying pulmonary disorders, radiologic findings (chest x-ray in 10 patients, CT in 8 patients, and ventilation scintigraphy in 1 patient; nuclear medicine studies were not indicated for the other patients, and PFTs were performed in 10 patients).

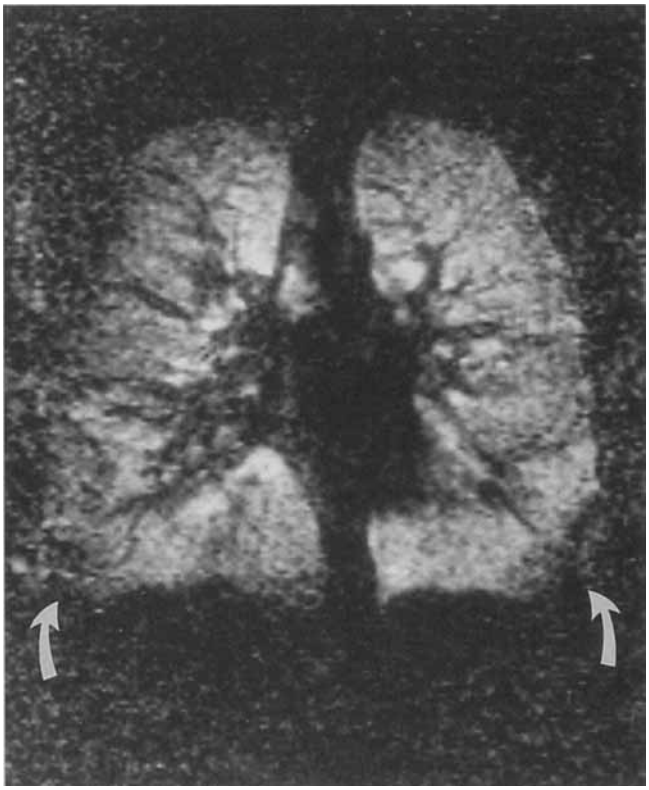

Figure 1. 3He MR image of the lung of a 32-year-old volunteer (nonsmoker) shows upper and lower lung fields with high signal intensity. The pulmonary vessels appear as structures without signal. Note the lateroinferior areas with low or no signal (curved arrows) due to spatial limitations of the circular Helmholtz coil.

• RESULTS

All studies of volunteers and 8 of 10 studies of patients were completed successfully. One patient did not tolerate the rehearsal of the inhalation procedure within the bore of the MR unit due to claustrophobia and dyspnea; no imaging study was performed. A second patient was not able to reproduce his (primarily achieved) breath-hold period of 24 seconds. After inhalation of the hyperpolarized sample, he held his breath for only 8 seconds. The images revealed hyperpolarized 3He gas within the lungs, but image quality was very poor with severe breathing artifacts, and the study was excluded. Four patients and two volunteers were not capable of breath-holding for the entire acquisition period but started to exhale during the last 5–8 seconds. In these cases, high signal was detected within the lungs and minor or moderate breathing artifacts were observed. These studies were not excluded from evaluation. Obvious cardiac motion artifacts were not observed in any case.

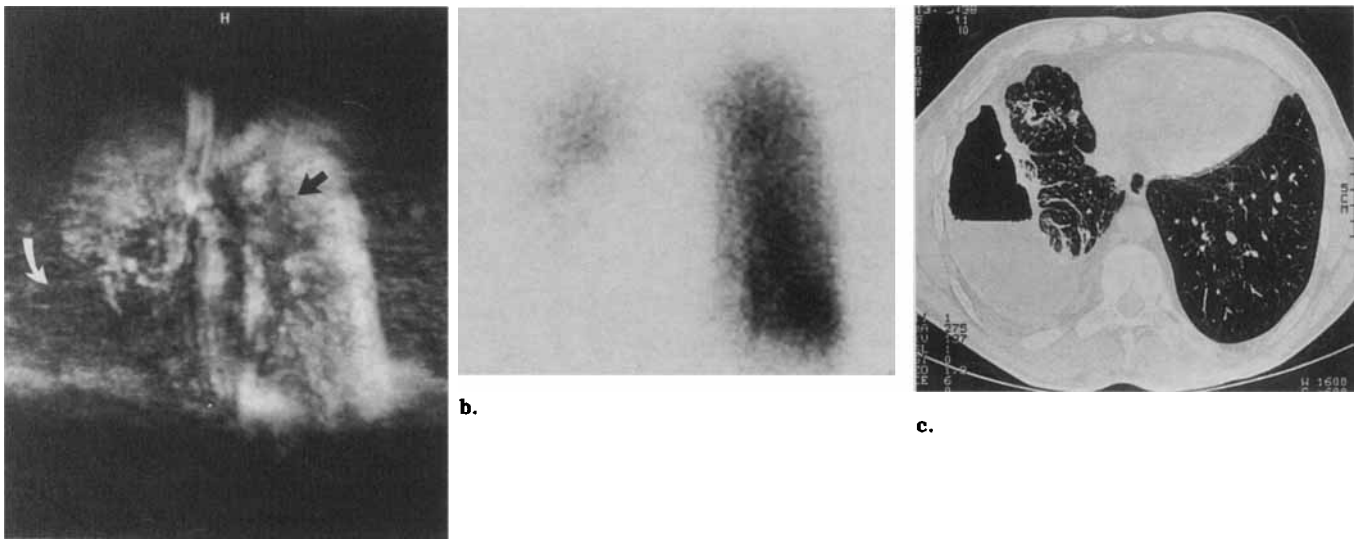

a. b. c.

Figure 2. Images of a 52-year-old patient with chronic empyema and a destroyed right lower lobe due to atypical tuberculosis. **(a)** 3He MRI MIP shows a large ventilatory defect in the right lower lobe (curved arrow). Note predominant ventilation of the peripheral subpleural airspaces on the left as compared with the central, parahilar areas (black arrow). Moderate breathing artifacts are present in the phase-encoding direction. **(b)** Corresponding ventilation scintigraphy confirms a large ventilatory defect in the right lower lobe and reduced ventilation in the upper right lobe as compared with the left lung. **(c)** Corresponding CT shows the chronic empyema with a air-fluid level and a destroyed right lower lobe.

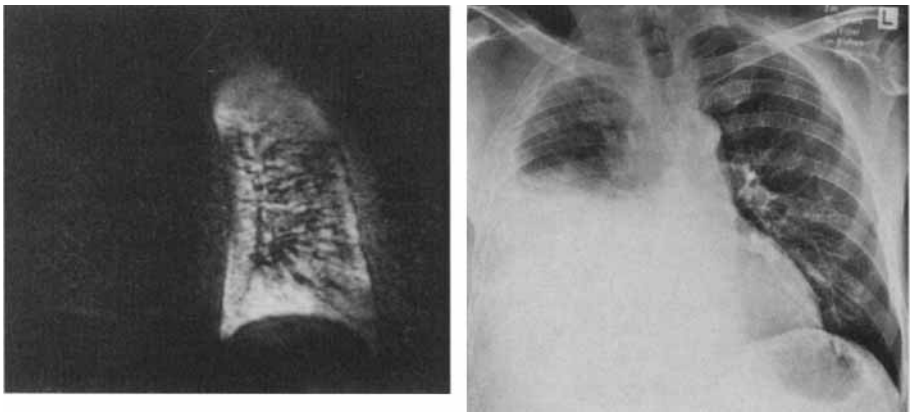

a. b.

Figure 3. Images of a 66-year-old patient with pleural effusion, bronchogenic carcinoma of the right main stem bronchus, and COPD. **(a)** 3He MRI obtained in the supine position shows only minimal ventilation of the right lung. Slight signal inhomogeneity in the left lung most likely represents ventilatory changes in COPD. **(b)** Corresponding chest x-ray (obtained in erect position the previous day) shows large pleural effusion and an aerated right upper lobe.

In six volunteers, there was no great difference in signal intensity between the upper and lower lung fields (Fig. 1). Five volunteers exhibited high signal intensity, and one exhibited intermediate signal intensity. In two volunteers, there was a predominance of the lower lung fields with high signal intensity, whereas the signal intensity in the upper lung fields was intermediate. In seven volunteers, the posterior lung fields exhibited high signal intensity, and one exhibited intermediate signal intensity. The anterior lung fields showed equally high signal intensity in four cases and intermediate signal intensity in four cases. The major fissure could be delineated in five cases. In four volunteers, peripheral wedge-shaped and curve-shaped areas (in the lower lateral lung fields) with low signal intensity were observed. Mild signal inhomogeneities were detected in two volunteers. The MIP images confirmed the almost complete and homogeneous ventilation of the lungs. All volunteers had normal PFTs.

In the patients, lung parenchyma not involved with focal disease showed high signal intensities in the upper (n = 6), lower (n = 8), anterior (n = 3), and posterior (n = 8) lung fields (Table 1). There was a predominance of the more peripheral, subpleural airspaces compared with the central areas in three patients (Figs. 2 and 3).

Chronic empyema (Fig. 2), bronchogenic carcinoma, bihilar lymphadenopathy, and pleural effusion (Fig. 3) resulted in large signal defects (Table 1). These areas with intermediate to no signal on 3He MRI appeared larger than the lesions on chest x-ray or CT, varying from an additional ring of a few millimeters around the mass to a signal defect of several centimeters distal or adjacent to the mass caused by compression or concomitant bronchial obstruction. The comparison with ventilation scintigraphy in the patient with the chronic empyema and the destroyed lobe due to atypical tuberculosis showed good correlation (Fig. 2). Both modalities revealed a large defect in the right lower lobe and little signal in the right upper lobe compared with the left lung. For the patient with carcinoma of the right main stem bronchus and large pleural effusion, 3He MRI (performed in the supine position) detected only minimum signal within the affected lung (Fig. 3). In contrast, the chest x-ray obtained in erect position the previous day showed evidence of an aerated right upper lobe. The difference between the chest x-ray

Table 1
Summary of Patient Data to Correlate Smoking History, CXR/CT Findings, History, and PFTs with the Predominant 3He MRI Finding and the Signal Intensity Detected in Different Parts of the Lung

No	Age (years)	Smoker	CXR/CT History	Lung Function	Predominant 3He MRI Finding	Signal Intensity Anterior	Posterior	Upper	Lower
1	66	Yes	PE, BC, COPD	Normal	Large defect	1	3	2	3
2	29	No	LNN	Normal	Large defect	2	3	2	3
3	50	Yes	BC, COPD	Obstruction	Large defect	3	3	3	3
4	52	No	Empyema	Combined	Large defect	1	3	3	3
5	50	Yes	COPD	Obstruction	Patchy pattern	2	3	3	3
6	61	Yes	COPD, Pneumonia	Obstruction	Patchy pattern, wedge-shaped defect	2	3	3	3
7	64	No	Bronchiectasis	Obstruction	Wedge-shaped defects	3	3	3	3
8	60	No	Fibrosis	Normal	Fine linear defects	3	3	3	3
9	70	Yes	COPD	Obstruction	Not successfully completed				
10	68	Yes	COPD	Obstruction	Dropout				

Note.—BC = bronchogenic carcinoma, COPD = chronic obstructive pulmonary disease, CXR = chest x-ray, LNN = lymph nodes. PE = pleural effusion, PFT = pulmonary function test, 1 = low, 2 = intermediate, 3 = high signal.

and the 3He MRI most likely represented the effect of posture with subsequent compression of the upper lobe by the pleural effusion in the supine position.

Patients with COPD (all of whom were smokers) showed both localized and diffuse signal inhomogeneities (Fig. 4). The extent of these findings was highly variable: the patient with the longest smoking history (60 pack years) exhibited the most severe inhomogeneities. Localized areas with very high signal intensity were found directly adjacent to areas with intermediate, low, or no signal resulting in a patchy pattern with a rather random distribution throughout both lungs. Only some intermediate signal intensity areas were wedge-shaped and located in the periphery of the lungs. For the patient with COPD and pneumonia, wedge-shaped defects were the predominant finding on the source images (Fig. 4a), but the MIP image also demonstrated the patchy pattern of COPD (Fig. 4b). Bronchiectasis, as confirmed by CT, resulted in multiple wedge-shaped defects in all lung fields that were equally well demonstrated on the source and the MIP images (Fig. 5). For the patient suffering from mild fibrosis due to systemic sclerosis, 3He MRI revealed almost unaffected ventilation showing only small defects in the lower lung fields. They corresponded well to the CT showing architectural distortion. Although morphologic alterations were present, ventilation was not significantly altered, which was confirmed by normal PFTs.

MIP images were superior to source images in the demonstration of ventilatory disturbances. This improvement was especially useful to illustrate patchy and wedge-shaped defects as well as random distribution in patients with COPD, pneumonia, or bronchiectasis. The extent and spatial distribution of ventilatory defects were even better illustrated by rotation of MIP images acquired with various projection angles as compared with source images or coronal MIPs alone. MIP images were inferior in the demonstration of large central defects due to superimposition by ventilated lung areas in the periphery.

Minor breathing artifacts without significant degradation of image quality were observed in two of eight volunteers and in four of eight patients. Breathing before completion of the acquisition was recognized by smearing in the phase-encoding direction caused by motion of the chest wall. Minor breathing artifacts were observed in five of six subjects. Moderate artifacts occurred in the examination of the patient with the chronic empyema (Fig. 2). Diaphragmatic motion may have occurred in the readout direction and did not result in artifacts. No obvious cardiac motion-related artifacts with areas of signal void in the regions adjacent to the heart were observed in any case.

• DISCUSSION

3He MRI is receiving increasing attention within the radiologic community because recent reports presented fascinating data (1–5). We report one of the first applications in patients. The results strongly support the high clinical expectations of 3He MRI. Homogeneous high signal within airspaces represents the normal 3He MRI finding in individuals without pulmonary disease. Patchy and wedge-shaped signal inhomogeneities, as well as large defects, represent the most frequent and important findings.

Although our technical setup is still quite experimental, the inhalation and imaging procedure was completed successfully by all healthy volunteers and most patients with lung diseases and impaired pulmonary function. Severe obstruction and reduced oxygen reserve may have been responsible for the two unsuccessful studies. Because patients are deprived of the inspiratory oxygen supply during the inhalation procedure (three breaths of helium) and the breath-hold period (>22 seconds), hypoxemia is not unlikely to occur. Therefore, we refrain from using 3He MRI in severely dyspneic patients for safety reasons, ie, to avoid asphyxia.

The amount of helium provided for the imaging studies (300 ml, 3×10^5 Pa, 35–45% polarized) was sufficient to fill the airspaces of healthy nonsmoking volunteers if properly inhaled. This amount is significantly smaller than the 750 ml used in other studies (5) because of the higher degree of polarization. Most volunteers showed a rather homogeneous distribution of the inhaled 3He gas. The direct visualization of airspaces by 3He MRI represents an important new development and a considerable complement of conventional proton MRI. Quantification, however, still has to be developed. The lower and posterior lung fields constantly showed high signal intensities, whereas the upper and anterior portions exhibited intermediate signal intensities in some cases. In the volunteer studies, the spatial limitations of our experimental transmit/receive coil were detected: the lateroinferior lung regions had been cut off. They represented the major drawback of image quality. Additionally, peripheral, subpleural airspaces (located near the loops of the coil) had higher signal than central areas in patients with a big chest. This difference in signal did not significantly bias the MIP findings. It probably was artifactual and represented another limitation of our coil. Contradictory findings (peripheral falloff in signal intensity) reported by MacFall using a smaller surface coil also were attributed to coil design (5). Regarding these limitations, we conclude that normal ventilation is represented by an almost complete and homogeneous distribution of the hyperpo-

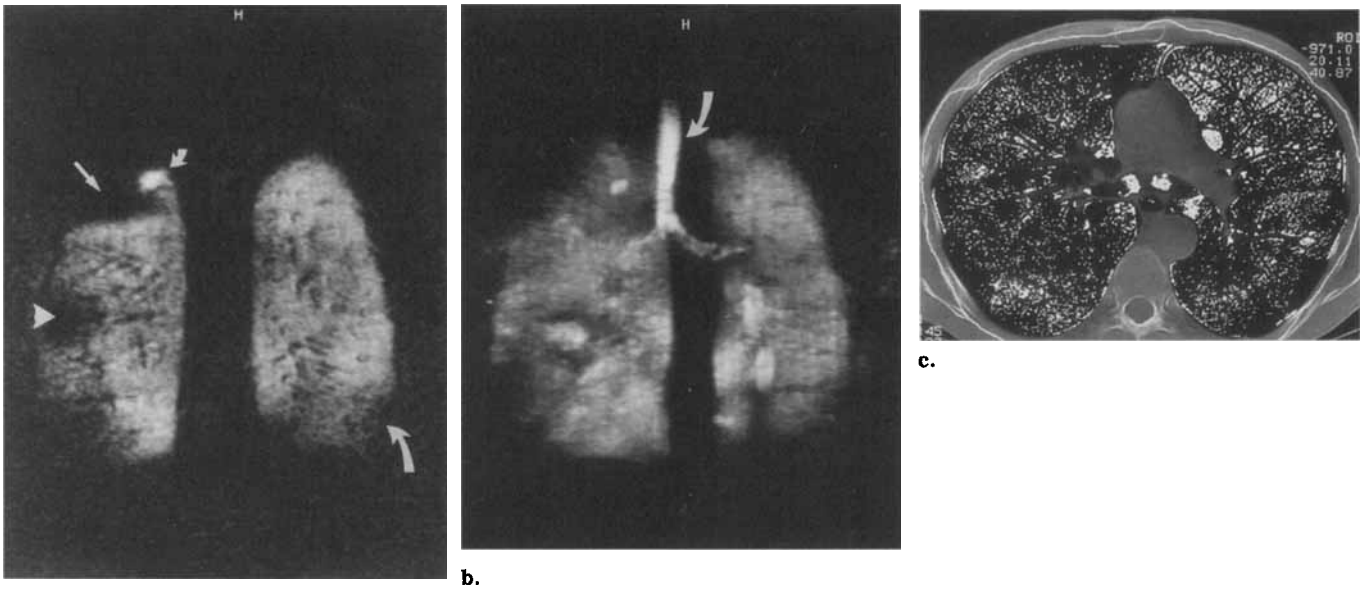

a. b. c.

Figure 4. Images of a 61-year-old patient with COPD and pneumonia. **(a)** 3He MRI shows signal inhomogeneity with hyperintense areas (small curved arrow) and wedge-shaped defects (arrowhead). The signal defect in the right upper lobe (straight arrow) is caused by pneumonia. Note also the curved signal defects at the lateroinferior lung regions due to the spatial limitations of the circular coil (curved arrow). **(b)** 3He MRI MIP shows high signal intensity in the trachea (curved arrow) and main stem bronchi with delineation of the cartilages. The MIP illustrates the marked signal inhomogeneities with a patchy pattern in both lungs due to COPD and emphysema. **(c)** Corresponding spiral CT with a density mask (threshold, −950 HU) to illustrate the extent of emphysema.

larized 3He gas. Improvements in coil and sequence design (2), as well as image normalization to compensate for RF field inhomogeneity of the coil, will lead to superior image quality and interpretability.

Signal defects and incomplete or inhomogeneous distribution of the hyperpolarized 3He gas were regarded as abnormal findings indicating ventilatory disturbances if technical defects were not suspected. Incomplete inhalation of the sample or breath-hold incapabilities of the patients may degrade image quality. The successful studies, however, suggest that even amounts smaller than 300 ml will be sufficient for 3He MRI of the pulmonary ventilation. They also show that the technique is quite robust with regard to the breath-hold capabilities of patients. Breathing during the later parts of the acquisition period did not result in a significant loss of signal. Motion artifacts slightly reduced image quality; abnormalities of pulmonary ventilation, however, still could be detected. Centric phase encoding could further reduce motion abnormalities.

Bronchogenic carcinoma, lymphadenopathy, chronic empyema, and pleural effusion caused signal defects by mass effect, which were larger than the lesions themselves. Therefore, 3He MRI did not provide morphologic information but visualized the subsequent ventilatory impairment that was more frequently suspected from 3He MRI than from other available imaging studies. The most striking 3He MRI findings were observed in patients with COPD, concomitant pneumonia, bronchiectasis, and a history of smoking. Moderate and severe signal inhomogeneities were depicted, indicating ventilatory disturbances. Areas with different signal intensities are likely to represent areas with different ventilatory levels or so-called compartments with different time constants with respect to ventilation. High signal intensity areas seem to be hyperventilated, representing fast compartments. Areas with low or no signal intensity indicate local hypoventilation and represent slow compartments. 3He MRI may be helpful to recognize and localize these different compartments, which cannot be achieved by any other modality. Therefore, 3He MRI might open new insights into pulmonary pathophysiology by localizing functional abnormalities. Regarding the distribution of signal inhomogeneities, two patterns can be differentiated: a patchy pattern and a wedge-shaped one. The patchy pattern is seen in patients with COPD and functional and/or radiologic evidence of emphysema as well as smoking history. It most likely indicates inhomogeneous ventilation due to bronchiolar disease, including respiratory bronchiolitis. The wedge-shaped pattern is seen in patients with COPD, concomitant pneumonia, and bronchiectasis. The areas with intermediate, low, or no signal most likely represent hypoventilation due to inspiratory bronchial obstruction, which may occur in acute and chronic bronchial infection. MIP images provided a better illustration of the extent and distribution of patchy and wedge-shaped defects than source images alone.

Regarding the findings in patients with COPD, we have to keep in mind that we visualized the inspiration of helium instead of ordinary air. It is not clear whether the findings can simply be transferred. It is likely that diffusion of helium within the small airways contributed significantly to the signal. Further investigations are needed to elucidate the role and the value of diffusion with respect to suppression of diffusion artifacts as well as diffusion-weighted 3He MRI. Another important factor is the interaction of hyperpolarized 3He and oxygen because of its paramagnetic properties. The direct contact of the two leads to rapid loss of polarization with a T1 of approximately 10 seconds at typical oxygen levels (10). For this reason, we started the inhalation procedure with ordinary 4He to partially wash out oxygen from the residual volume and to avoid or at least postpone direct contact between hyperpolarized 3He and oxygen. Therefore, T1 was prolonged to approximately 35 seconds, matching the acquisition period. It is important to realize that every RF excitation depletes polarization from the hyperpolar-

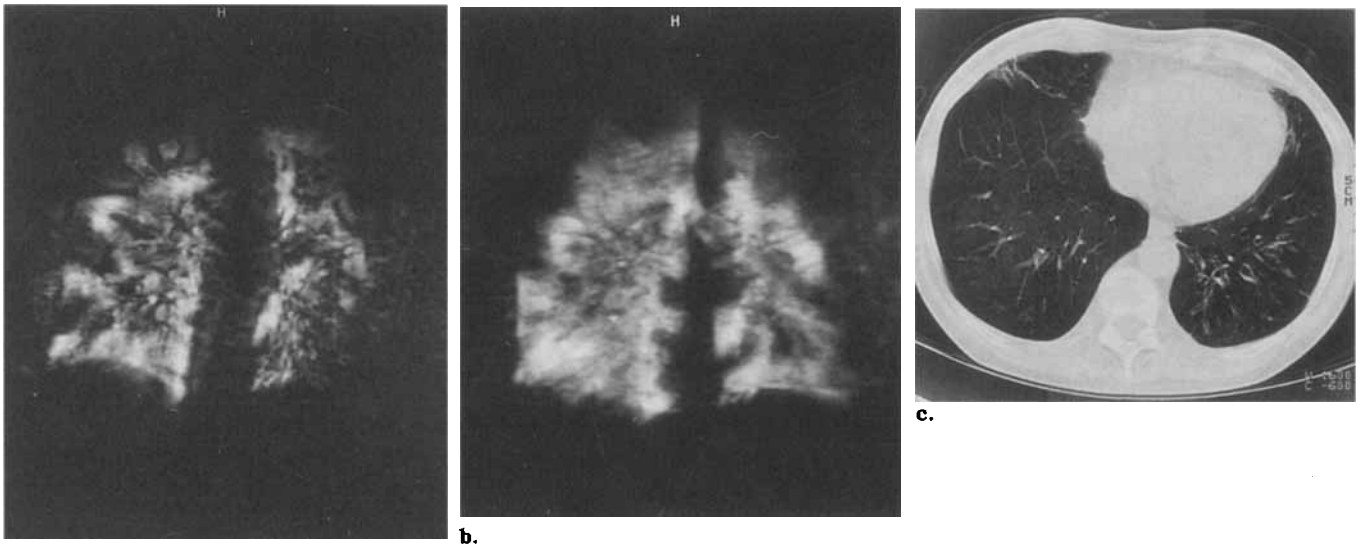

a. **b.** **c.**

Figure 5. Images of a 64-year-old patient with bronchiectasis. **(a)** 3He MRI of the posterior lung regions shows marked signal inhomogeneities with multiple wedge-shaped defects in both lungs, indicating ventilatory compromise due to bronchiectasis, particularly at the lung base on the left. **(b)** 3He MRI MIP illustrates the marked signal inhomogeneity with the wedge-shaped pattern in both lungs, which is also present in the right middle lobe. Note also the intermediate signal intensity in the trachea. **(c)** Corresponding spiral CT shows bronchiectasis, especially in the basal segments of the left lower lobe.

ized 3He sample, which cannot be replenished. Consequently, we performed only one acquisition per 3He sample inhaled. Imaging after expiration and dynamic studies of the whole breathing cycle are planned.

From our experience, we are convinced that 3He MRI is able to accurately visualize profound changes in pulmonary ventilation in patients with COPD. It seems likely that different types and locations of airway obstructions can be differentiated. In the clinical context, 3He MRI may be helpful in the assessment of patients with emphysema and COPD who are undergoing thoracic surgery for malignant disease or in the preoperative workup of candidates for volume-reduction surgery and lung transplantation. Further developments and more experience are needed to improve equipment and pulse sequences as well as to evaluate the potential clinical value of 3He MRI as compared with ventilation scintigraphy.

Acknowledgments: The authors thank Michael Deimling, Alexander Potthast, and Wilhelm Dürr, of Siemens Medical Systems, Erlangen, Germany, for their continuous support; Schott Glaswerke, Mainz, Germany, for the development of the iron-free supremax glass cells; Michèle Leduc, Ecole Normale Supérieure, Paris, for providing the laser technology for optical pumping of 3He; Peter Bachert, Michael Bock, Lothar Schad, and Michael V. Knopp, from the German Cancer Research Center, Heidelberg, Germany, for their fruitful cooperation; and Martin Buchenroth and Berthold Fischer, Department of Pneumology, Johannes Gutenberg-University of Mainz, Mainz, Germany, for patient care.

References

1. Middleton H, Black RD, Saam B, et al. MR imaging with hyperpolarized 3He gas. Magn Reson Med 1995; 33:271–275.
2. Black RD, Middleton HL, Cates GD, et al. In vivo He-3 MR images of Guinea pig lungs. Radiology 1996; 199:867–870.
3. Ebert M, Grossmann T, Heil W, et al. Nuclear magnetic resonance imaging on humans using hyperpolarized 3He. Lancet 1996; 347:1297–1299.
4. Bachert P, Schad L, Bock M, et al. Nuclear magnetic resonance imaging of airways in humans with use of hyperpolarized 3He. Magn Reson Med 1996; 36:192–196.
5. MacFall JR, Charles HC, Black RD, et al. Human lung air spaces: potential for MR imaging with hyperpolarized He-3. Radiology 1996; 200:553–558.
6. Eckert G, Heil W, Meyerhoff M, et al. A dense polarized 3He target based on compression of optically pumped gas. Nucl Instr Methods Phys Res 1992; A320:53–65.
7. Heil W, Surkau R. Development of a dense polarized 3He spin filter based on compression of optically pumped gas. J Neutron Res 1997 (in press).
8. Heil W, Humblot H, Otten E, Schäfer M, Surkau R, Leduc M. Very long nuclear relaxation times of spin polarized helium3 in metal coated cells. Physics Letters 1995; A201:337–343.
9. Kauczor H-U, Hofmann D, Kreitner K-F, et al. 3He MRI of normal and abnormal pulmonary ventilation: visualization using inhalation of hyperpolarized 3He gas. Radiology 1996; 201: 564–568.
10. Saam B, Happer W, Middleton H. Nuclear relaxation of 3He in the presence of O2. Physiol Rev 1995; A52:862–865.